J|A|C|S
ARTICLES

Published on Web 03/10/2010

Electrically Driven Redox Process in Cerium Oxides

Peng Gao,[†] Zhenchuan Kang,[‡] Wangyang Fu,[†] Wenlong Wang,[†] Xuedong Bai,*[,†] and Enge Wang*[,†,§]

Beijing National Laboratory for Condensed Matter Physics, Institute of Physics, Chinese Academy of Sciences, Beijing 100190, China, RE-POWER TECH, 8211 E. Garfield Street, Scottsdale, Arizona 85257, and School of Physics, Peking University, Beijing 100871, China

Received October 12, 2009; E-mail: xdbai@aphy.iphy.ac.cn; egwang@pku.edu.cn

Abstract: Cerium oxides have attracted much attention because of their uses in three-way catalysts and other catalyst applications. The redox reaction of cerium oxides, as the basis of their use as catalysts, usually takes place at high temperature (>600 K) and/or low oxygen partial pressure. There have been continuous efforts to lower the operating temperatures of cerium oxide further to improve the performance of the catalysts and reduce pollution under the cold-start condition. Here, we report a direct atomic-scale observation of a redox process in cerium oxides driven by an electrical field at ambient temperature. The dynamic changes taking place during the electrically driven redox reaction were imaged by in situ high-resolution transmission electron microscopy, where reversible phase transformations due to the migration of oxygen vacancies have been reproducibly achieved. These results could lead to the low-temperature operation of catalysts for the purification of automobile emissions of pollutants, oxygen generation, and intermediate-temperature solid oxide fuel cells.

Introduction

Automobile pollution is one of the factors contributing to global warming. One solution for reducing pollution is to lower the operating temperature of the catalysts for the purification of automobile-emitted pollutants. Cerium oxides have attracted much attention because of their uses in the three-way catalyst (TWC) and other catalyst applications.[1−3] A redox reaction (releasing and storing oxygen) is the basic process for ceria catalytic applications. The redox activity of the catalysts depends on the operating temperatures and oxygen partial pressure. In the past decade, the low-temperature redox activity and stability of cerium oxides have been improved for TWC application by incorporating zirconia and rare earth oxides.[4−10] The redox process involves the phase transformation of cerium oxide and is usually attainable at a temperature >600 K. The emissions of pollutants are high during the cold start of a combustion engine until the catalyst reaches high operating temperatures.[10] There have been continuous efforts to further lower the operating temperatures of cerium oxide to reduce pollution under the cold-start condition.

Cerium oxides have cubic fluorite structure, in which the cation sublattice is a superstable frame because of ionic bonding.[11] Cerium oxides have high melting temperatures (>2500 K) because of their cubic fluorite structure.[12] However, oxygen anions in cerium oxide are very active and have high mobility even at temperatures as low as 573 K, resulting in redox cycles under low oxygen partial pressures.[13] Cerium oxide tends to create anion deficiencies, and the oxygen vacancies can move though the lattice relatively easily[4,5] because of the character of the fluorite structure and the electronic configuration ($[Xe]4f^15d^16s^2$) of Ce atoms.[14] Recently, a reversible phase transformation of ceria taking place at 1003 K in a hydrogen atmosphere has been found by using in situ environmental transmission electron microscopy (TEM).[15] It is directly observed that the introduced oxygen vacancies give a cubic superstructure during the reduction processes.

Here, we report on the reversible redox reactions in cerium oxides driven by an electrical field at ambient temperature, studied by in situ electrical probe TEM, where the structural evolutions of cerium oxides on the atomic scale are simultaneously recorded when an electrical field is periodically applied across the oxides. It is shown that the redox process in cerium oxides can be driven by an electrical field instead of elevated temperature.

[†] Chinese Academy of Sciences.
[‡] RE-POWER TECH.
[§] Peking University.

(1) Deluga, G. A.; Salge, J. R.; Schmidt, L. D.; Verykios, X. E. *Science* **2004**, *303*, 993–997.
(2) Park, S. D.; Vohs, J. M.; Gorte, R. J. *Nature* **2000**, *404*, 265–267.
(3) Otsuka, K.; Ushiyama, T.; Yamanaka, I. *Chem. Lett.* **1993**, 1517–1520.
(4) Trovarelli, A. *Catal. Rev.—Sci. Eng.* **1996**, *38*, 439–520.
(5) Mogensen, M.; Sammes, N. M.; Tompsett, G. A. *Solid State Ionics* **2000**, *129*, 63–94.
(6) Liu, W.; Sarofim, A. F.; Flytzani-Stephanopoulos, M. *Appl. Catal., B* **1994**, *4*, 167–186.
(7) Kang, Z. C.; Eyring, L. *J. Solid State Chem.* **2000**, *155*, 129–137.
(8) Fornasiero, P.; Dimonte, R.; Rao, G. R.; Kaspar, J.; Meriani, S.; Trovarelli, A.; Graziani, M. *J. Catal.* **1995**, *151*, 168–177.
(9) Rao, G. R.; Kaspar, J.; Meriani, S.; Dimonte, R.; Graziani, M. *Catal. Lett.* **1994**, *24*, 107–112.
(10) Shelef, M.; McCabe, R. W. *Catal. Today* **2000**, *62*, 35–50.
(11) Wang, Z. L.; Kang, Z. C. *Functional and Smart Materials: Structural Evolution and Structure Analysis*; Plenum Press: New York, 1998.
(12) Adachi, G.; Imanaka, N. *Chem. Rev.* **1998**, *98*, 1479–1514.
(13) Bevan, D. J. M.; Kordis, J. *J. Inorg. Nucl. Chem.* **1964**, *26*, 1509–1523.
(14) Kang, Z. C. *Handbook on the Physics and Chemistry of Rare Earths*; Elsevier: Amsterdam, 2008; Vol. 38.
(15) Crozier, P. A.; Wang, R. G.; Sharma, R. *Ultramicroscopy* **2008**, *108*, 1432–1440.

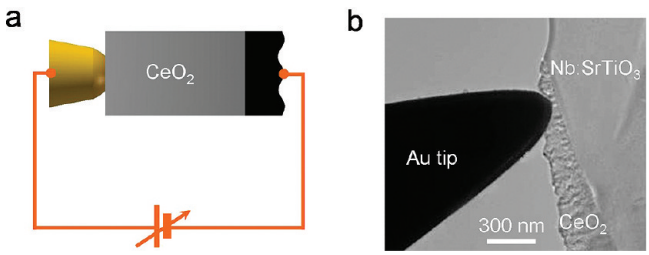

Figure 1. (a) Scheme of the experimental setup. (b) In situ TEM image of the gold-tipped CeO_2 film−conductive substrate structure. An epitaxial CeO_2 film was deposited on a Nb-doped $SrTiO_3$ (Nb/STO) substrate.

Experimental Methods

The high oxides of cerium (CeO_2) films were grown by pulsed-laser deposition (PLD) on $SrTiO_3$ (Nb doping at 0.7 wt %) substrates, which were very electrically conductive. The TEM cross-sectional samples were prepared by conventional mechanical polishing and argon ion milling. (See the details in Supporting Information (SI)). These samples were then loaded into a homemade specimen holder. An electrochemically etched gold tip was used as the movable electrode that makes electrical contact with the cerium oxide films. The conductive substrate of the film acts as the counter electrode. Thus, an electrical field can be applied across the CeO_2 film, as shown in Figure 1.

Results and Discussion

In the absence of an electrical field, the HRTEM image and electron diffraction pattern along the ⟨110⟩ zone axis of CeO_2 was recorded, as shown in Figure 2a. When a bias was applied to the sample, structural changes became obvious as we increased the voltage. Figure 2b displays the HRTEM image from the same region of Figure 2a at a bias of 6 V (electrical field $E \approx 8 \times 10^7$ V/m). This image shows the structural transformation with the appearance of the sweeping of the modulation wave across the oxide film. (See the movie in SI.) Extra diffraction spots were also observed under the applied electrical field (inset of Figure 2b). These superlattice reflections indicate that oxygen anions have been removed from the CeO_2 film and the introduced oxygen vacancies were structurally ordered as Ce_2O_3.[15–17] As a rare earth high oxide, the surfaces of CeO_2 are chemically and physically active,[18] where oxygen anions have a lower binding energy because of the asymmetric interaction with cations. As an electrical field is applied to the CeO_2 crystal, oxygen anions at the surface will be attracted

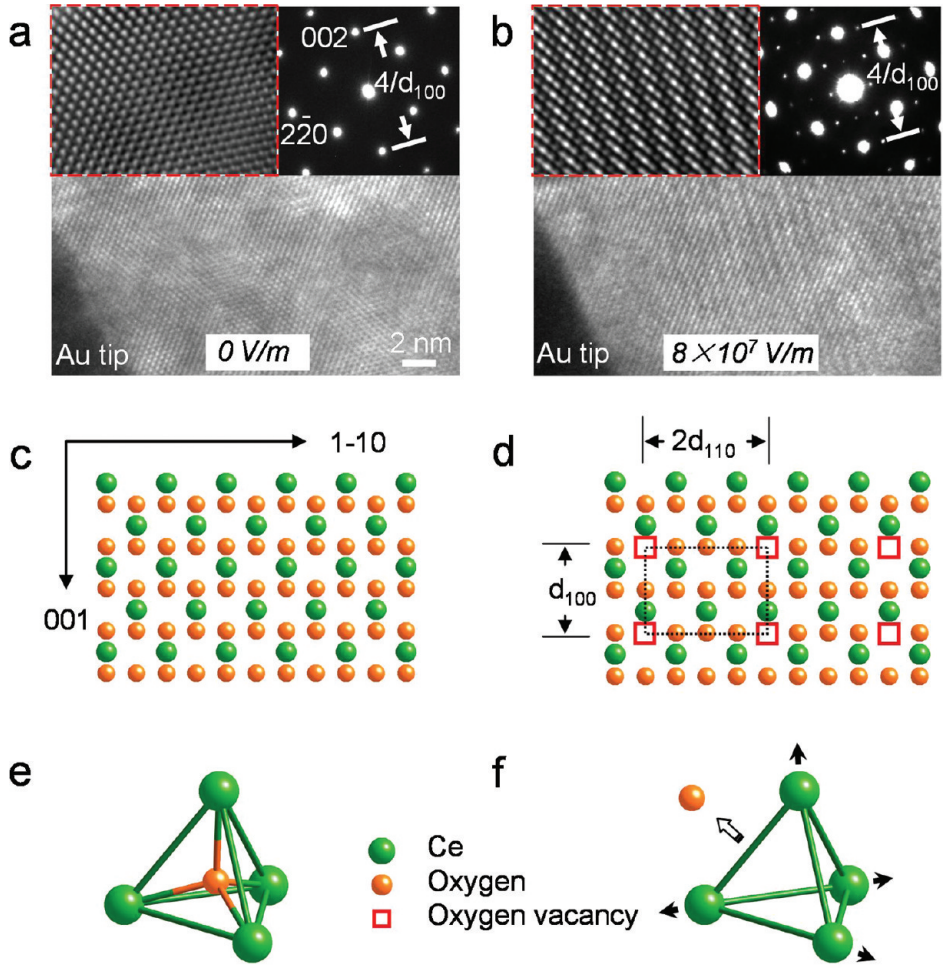

Figure 2. (a) In situ TEM image of a single-crystal CeO_2 film along the ⟨110⟩ zone axis. The enlarged HRTEM image and the corresponding SAED pattern are shown in the upper left and the upper right insets, respectively. d_{100} is the interplanar spacing of the (100) plane of CeO_2. (b) The wave-sweeping patterns appeared when a bias of 6 V ($E \approx 8 \times 10^7$ V/m) was applied across the CeO_2 film, indicating the decomposition of the cerium oxide. Superlattice reflections (upper left) and extra diffraction spots (upper right) were observed in this case. (c) Solid-sphere model of CeO_2 in a perfect fluorite structure. This drawing represents the projection along the ⟨110⟩ direction. (d) Solid-sphere model showing the formation of oxygen vacancies. The rectangles indicate the vacancy superlattices. (e) Cerium oxide can be viewed as tetrahedrals with cations at the corners and oxygen anions at the centers. (f) Cerium oxide with an oxygen vacancy will cause the CeO_2 film cations to repel each other because of coulomb interactions. The arrowhead indicates the displacement direction of the oxygen anion.

toward the positive electrode and driven out of the surface. Similarly, anions that are present inside the film will also be attracted and move toward the surface. This means that oxygen vacancies will be formed and will diffuse in a reversed direction and propagate into the interior of the crystal. These oxygen vacancies will cause the corrugation of two adjacent cation packing layers as the original oxygen anions leave the lattice. This will attract other negatively charged oxygen anions toward the vacancies and will lead to a series of migrations as the local positive charges at the vacancy sites are compensated for by adjacent oxygen anions. Thus, the oxygen migration process can be viewed as a continuous diffusion of the anions.

The appearance of the sweeping of the modulation wave indicates that the introduced oxygen vacancies became ordered by the driving of the applied electrical field. CeO_2 was finally reduced to Ce_2O_3. The structural model for the process of forming ordered oxygen vacancies is represented in Figure 2c−f. The rectangle in Figure 2d shows the unit cell of the sesquioxide of cerium oxide in the ⟨110⟩ orientation resulting from ordered oxygen vacancies. When a vacancy is created, the neighboring cations will repel each other along the direction indicated in Figure 2f because of coulomb interactions. Thus, the distance between cations will increase, forming a pathway for the migration of oxygen anions. This model is the basis of fast oxygen diffusion in cerium oxide. Our experimental results (insets of Figure 2a,b) showed that $d^a_{100}/d^b_{100} = 97\%$, implying that the phase transformation from high oxygen content (a, CeO_2) to low oxygen content (b, Ce_2O_3) was accompanied by a volume increase.[19,20] The vacancies can be recovered reversibly by the residual oxygen gas in the TEM chamber (oxygen partial pressure of around 10^{-5} Pa) after removing the electrical field, and the Ce_2O_3 film was reoxidized with the disappearance of the superstructure. Multiple cycles of the reduction process driven by an electrical field and then reoxidation by the residual oxygen gas in the TEM chamber have been reproducibly recorded. (See the movie in SI.)

Electron energy loss spectroscopy (EELS) measurements were carried out to further confirm the reduction and oxidation process of the cerium oxide film. Figure 3 shows the Ce−M edge (Figure 3a) and O−K edge (Figure 3b) of the EELS spectra obtained from cerium oxide before (spectrum 1) and after (spectrum 2) applying the electrical field. Spectrum no. 3 was recorded after removing the applied electrical field. A reversal in the intensity of $Ce-M_{45}$ white lines (between 1 and 2 in Figure 3a) shows that Ce has undergone a transition from the 4+ to 3+ oxide state[21] under the applied electrical field. With the applied electrical field, the disappearance of the shoulder (arrowhead at spectrum 1 in Figure 3a) suggests that the strong covalent hybridization between the Ce 4f and O 2p states[22] disappeared by applying an electrical field. From the O−K edge spectra (Figure 3b), the intensity of peak A (~530 eV), which

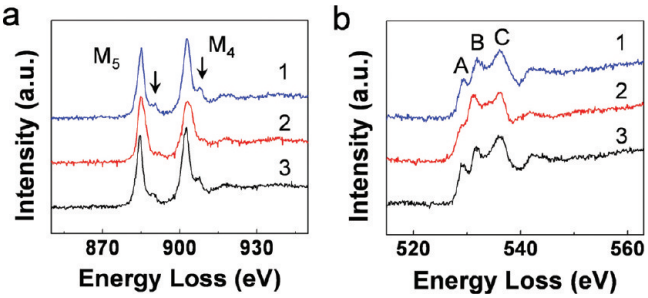

Figure 3. (a) EELS spectra of the Ce−M edge. Spectrum 1 was taken from the original CeO_2 film. A reversal in the intensity of $Ce-M_4$ and $Ce-M_5$ white lines was found when applying an electrical field (spectrum 2) and was recovered after removing the electrical field (spectrum 3). The shoulder in spectrum 1 also disappeared under the applied electrical field, as indicated in spectrum 2. (b) EELS spectra showing the O−K edge obtained from the cerium oxide film before (spectrum 1) and after (spectrum 2) applying the electrical field. Peak A (~530 eV) of spectrum 1, corresponding to the unoccupied Ce 4f/O 2p hybridization, disappeared after applying the electrical field (spectrum 2) and was recovered after removing the electrical field (spectrum 3).

corresponds to unoccupied Ce 4f/O 2p hybridization,[23] decreased after the electrical field was applied, indicating the formation of oxygen vacancies associated with the usual exchange of Ce^{4+} in CeO_2 with unoccupied extended Ce 4f states in Ce^{3+} with an occupied, localized, corelike 4f state.[24] In perfect CeO_2, every oxygen atom is situated in the center of a tetrahedron, surrounded by four Ce atoms. The oxygen p orbital has two extra electrons provided by a Ce atom. When an oxygen atom is leaving its lattice position, these electrons may occupy the lowest possible empty state, which is the f orbital of the nearest Ce atoms, tuning Ce^{4+} to Ce^{3+}. When the vacancies were recovered, these electrons were localized on cerium atoms in the surroundings of the vacancies and, correspondingly, they were delocalized and transferred to oxygen from Ce sites again, as displayed by EELS spectra no. 3 in which the Ce oxidation state immediately reverted to 4+.

It is noted that, although Joule heating and TEM electron irradiation may cause a phase transformation,[15] both of them can be ruled out in our in situ TEM studies. (See the details in SI.)

To understand the mechanism of the electrically driven redox process of cerium oxides, the oxygen vacancy migrations were recorded inside HRTEM, as shown in Figure 4a,b. Under the applied electrical field, the oxygen anions are activated to migrate because of the lowered barrier, as depicted in Figure 4c,d. The oxygen vacancies that formed at the surface migrated to the cathode and then assembled, so the cerium oxide near the cathode was first reduced to Ce_2O_3 and the superstructure strips emerged near the cathode. When more and more oxygen anions were left, the superstructure strips propagated to the anode. In the beginning, the higher oxide of cerium is put into an equilibrium state with oxygen molecules in the gas phase. The oxygen chemical potential (μ_O) is closely related to the equilibrium stability, described as a function of temperature (T) and oxygen partial pressure (p),[11]

$$\mu_O = \mu_O^0 + RT \ln(p/p^0)$$

(16) Sharma, R.; Crozier, P. A.; Kang, Z. C.; Eyring, L. *Philos. Mag.* **2004**, *84*, 2731–2747.
(17) Akita, T.; Okumura, M.; Tanaka, K.; Kohyama, M.; Haruta, M. *Catal. Today* **2006**, *117*, 62–68.
(18) Esch, F.; Fabris, S.; Zhou, L.; Montini, T.; Africh, C.; Fornasiero, P.; Comelli, G.; Rosei, R. *Science* **2005**, *309*, 752–755.
(19) Wolcyrz, M.; Kepinski, L. *J. Solid State Chem.* **1992**, *99*, 409–413.
(20) Perrichon, V.; Laachir, A.; Bergeret, G.; Frety, R.; Tournayan, L.; Touret, O. *J. Chem. Soc., Faraday Trans.* **1994**, *90*, 773–781.
(21) Garvie, L. A. J.; Buseck, P. R. *J. Phys. Chem. Solids* **1999**, *60*, 1943–1947.
(22) Finazzi, M.; deGroot, F. M. F.; Dias, A. M.; Kappler, J. P.; Schulte, O.; Felsch, W.; Krill, G. *J. Electron Spectrosc. Relat. Phenom.* **1995**, *78*, 221–224.
(23) Hu, Z.; Meier, R.; Schussler-Langeheine, C.; Weschke, E.; Kaindl, G.; Felner, I.; Merz, M.; Nucker, N.; Schuppler, S.; Erb, A. *Phys. Rev. B* **1999**, *60*, 1460–1463.
(24) Skorodumova, N. V.; Simak, S. I.; Lundqvist, B. I.; Abrikosov, I. A.; Johansson, B. *Phys. Rev. Lett.* **2002**, *89*, 166601.

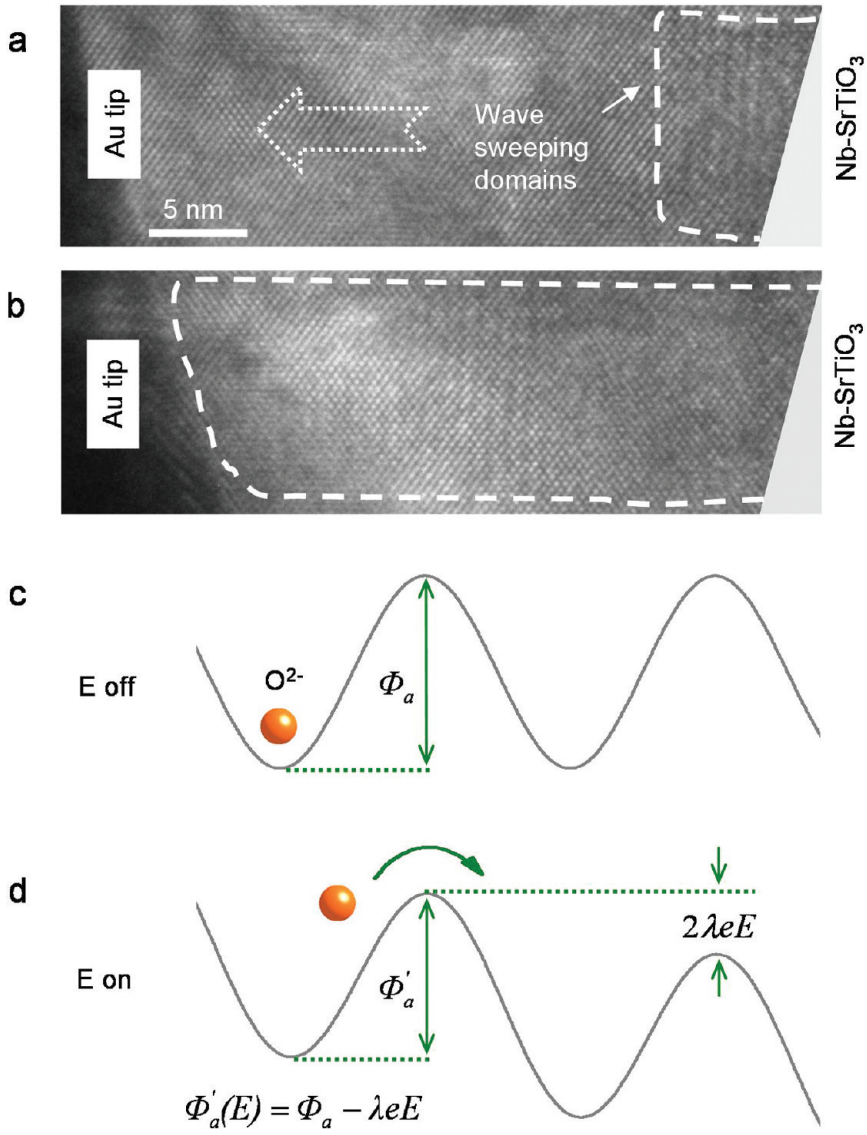

Figure 4. TEM images showing that the sweep of the modulation wave first emerged at the cathode (a) and then propagated through the cerium oxide film to the anode (b), indicated by the large arrowhead. The small, thin arrowhead points to the wave sweeping region, corresponding to the Ce^{3+} region. (c, d) Schematics of the electrical field effect. Top: no electrical field and oxygen anions in the crystal. Bottom: under the electrical field, the barrier was lowed. The anions could easily move to the anode. Φ_a is the activation energy, Φ'_a is the bias-dependent activation energy, λ is the jump length of the anions, and E is the electrical field when a bias is applied.

where μ_O^0 is the standard chemical potential of oxygen, R is the gas constant, and p^0 is the standard pressure of 1 atm.

In the presence of an electrical field, the equilibrium is determined by both the oxygen chemical potential and the electrical potential. The electrochemical potential is[25]

$$\tilde{\mu}_O = \mu_O^0 + RT \ln(p/p^0) + ZF\varphi$$

where Z is 1 for an electron or 2 for an oxygen anion, F is Faraday's constant, and φ is the electrostatic potential. The electrochemical potential determines the migration of anions. During this process, the electrons are supplied by one electrode and transform Ce^{4+} into Ce^{3+} and simultaneously take an electron from oxygen anion O^{2-} to oxidize it into an O atom with other electrode. We have estimated the critical electrical potential for the reduction of CeO_2. The release of oxygen usually takes place at a very low oxygen partial pressure, for instance, 10^{-26} Pa at ~923 K.[13] In this study, we assume that the sample is at room temperature and under 2×10^{-5} Pa vacuum. Thus, we can estimate that the critical electrical potential is about 2.8 V. The density function theory calculation also showed that the oxygen vacancy formation energy is in the region of 2.35−4.55 eV by using different functions.[24,26] In our experiments, by increasing the bias, the phase transition can be much more easily observed. When the electrical field is removed, the thermodynamic equilibrium state is broken and the oxygen content of the cerium oxide goes back to the case before the electrical field was applied. It is the electrostatic potential that plays a key role in the phase transformation of cerium oxides.

(25) Ashcroft, N. W.; Mermin, N. D. *Solid State Physics* ; Holt, Rinehart and Winston: New York, 1976.

(26) Jiang, Y.; Adams, J. B.; van Schilfgaarde, M.; Sharma, R.; Crozier, P. A. *Appl. Phys. Lett.* **2005**, *87*, 141917.

Conclusions

Our study shows the direct atomic-scale observation of an electrically driven redox process in cerium oxide films. In addition to the temperature and oxygen partial pressure, the electrical field is verified to be a new parameter that can efficiently induce the phase transformation of cerium oxides. A large number of oxygen atoms can be released and stored in cerium oxides, driven by electrical fields. These results may have a great impact on ceria-based catalysts, of which the working temperature can be decreased by an electrical field to overcome the cold-start problem of internal combustion engines. Beyond catalysis, the electrically driven redox reaction of cerium oxides may open a way to new, performance-improved applications in fuel cells, oxygen pumps, solid-state electrolytes, and ionic conductors.

Acknowledgment. We are grateful for financial support from the NSF (grant nos. 60621091, 10874218, and 50725209), MOST (grant nos. 2009DFA01290, 2007CB936203, and 2007AA03Z353), and CAS of China.

Supporting Information Available: Experimental details and supplementary figures. This material is available free of charge via the Internet at http://pubs.acs.org.

JA9086616